

Supplementary Materials for

Klotho May Ameliorate Proteinuria by Targeting TRPC6 Channels in Podocytes

Ji-Hee Kim,¹ Jian Xie,^{2,#} Kyu-Hee Hwang,^{1,#} Yueh-Lin Wu,^{2,6} Noelynn Oliver,³ Minseob Eom,⁴ Kyu-Sang Park,^{1,5} In Deok Kong,^{1,5} Chou-Long Huang,^{2,¶} and Seung-Kuy Cha^{1,5,¶}

¹Departments of Physiology and Global Medical Science, Yonsei University Wonju College of Medicine, Wonju, Republic of Korea; ²Division of Nephrology, Department of Internal Medicine, UT Southwestern Medical Center, Dallas, Texas, USA; ³Cardiometabolic Disease Research, Boehringer Ingelheim Pharmaceuticals, Inc. Ridgefield, CT, USA; ⁴Department of Pathology, Yonsei University Wonju College of Medicine, Wonju, Republic of Korea; ⁵Institute of Lifestyle Medicine, Yonsei University Wonju College of Medicine, Wonju, Republic of Korea; ⁶Division of Nephrology, Department of Internal Medicine, Taipei Medical University Hospital, Taipei, Taiwan

Supplementary Text

Klotho does not affect intrinsic channel properties of TRPC6. Cultured podocytes are flattened cells with relatively high membrane capacitance indicative of a large cell size. This feature creates space-clamp errors preventing accurate biophysical analysis of channel properties using voltage-clamp electrophysiological recordings (1). Thus, we investigated the intrinsic channel properties of TRPC6 regulated by klotho using heterologous expression in HEK293 cells that are much smaller in size. We measured TRPC6-mediated currents in response to carbachol (CCh) by whole-cell patch-clamp recording in HEK cells co-transfected with TRPC6 and $G_{\alpha_{q/11}}$ -coupled M_3 muscarinic receptor (Supplementary Figure 2A). HEK cells expressing recombinant TRPC6 and M_3R exhibit characteristic doubly rectifying TRPC6 currents in response to CCh (Supplementary Figure 2D). TRPC6-mediated currents were not detected in the co-transfected cells without CCh, and nor in mock-transfected cells with or without CCh (not shown). Soluble klotho inhibited CCh-activated TRPC6 current density (Supplementary Figure 2B), but did not alter activation kinetics examined by the half-time to maximal activation ($t_{1/2}$) (inset in Supplementary Figure 2A and Supplementary Figure 2C). While the amplitude of CCh-activated TRPC6 currents was reduced by soluble klotho, voltage-current (I-V) relationship curves for scaled-up relative currents with or without klotho were completely superimposable (Supplementary Figure 2, D and E). As in podocytes, klotho reduced OAG-activated TRPC6 channel activity (Supplementary Figure 2, F and G). These results showing lack of effects on activation kinetics and I-V relationship curves support the notion that klotho does not affect intrinsic channel properties of TRPC6.

Klotho reduces cell surface abundance of TRPC6 in podocytes by inhibiting PI3K-dependent exocytosis of the channel. We have found that klotho downregulates TRPC6 in cardiomyocyte by inhibiting PI3K-dependent exocytosis of the channel (2). We asked whether similar mechanism may contribute to the inhibition of TRPC6 by klotho in podocytes

and further investigated the signaling cascade downstream of activation of PI3K. Cell surface abundance of TRPC6 measured by biotinylation was markedly increased in the presence of serum relative to in serum-free medium and the increase was blocked by pre-incubation with brefeldin A (BFA) or tetanus toxin (TeNT) to disrupt vesicular exocytosis (Supplementary Figure 3A). These findings of surface abundance measurement were confirmed by Ca^{2+} imaging experiment showing that ATP-induced Ca^{2+} influx was blunted by BFA or TeNT (Supplementary Figure 3, B and C). TeNT cleaves VAMP2 (vesicle-associated membrane protein 2), a vSNARE, to block exocytosis of vesicles. ATP-induced increases in $[Ca^{2+}]_i$ were blunted by knockdown of endogenous VAMP2 in podocytes (Supplementary Figure 3, D-F). These latter findings were corroborated by the results that surface abundance of TRPC6 was decreased by knockdown of VAMP2 (Supplementary Figure 3G). These results support the notion that serum growth factors stimulate exocytosis of TRPC6 in podocytes.

Nest, we found soluble klotho decreased ATP-induced increases in $[Ca^{2+}]_i$ (Supplementary Figure 4A). Inhibition of PI3K by preincubation with wortmannin (WMN) decreased ATP-induced increases in $[Ca^{2+}]_i$ and prevented the soluble klotho-mediated decreases (Supplementary Figure 4, A and B). Similar findings were observed using a different inhibitor of PI3K, LY294002 (not shown). One of the downstream events consequent to stimulation of PI3K is phosphorylation of Akt at a threonine residue in the T-loop as well as a serine residue in the hydrophobic motif leading to its activation. As shown by western blot analysis of p-Akt(S), serum stimulated phosphorylation of Akt in podocytes, and soluble klotho blocked the stimulation (Supplementary Figure 4C). Collectively, these data support the notion that soluble klotho inhibits PI3K-Akt-dependent exocytosis of TRPC6 in podocytes.

Soluble klotho also inhibits TRPC3 channels that may associate with TRPC6.

Members of TRPC family co-assemble in multiple potential combinations when co-

expressed in cultured cells, which may give rise of channels of mixed regulatory and biophysical properties (3). The precise composition of channel complexes in podocytes that include TRPC6 as a subunit remains elusive. We detected mRNA transcript of *Trpc2*, *c3*, *c5*, and *c6* channels in differentiated cells of the immortalized mouse podocyte cell line used in the study (Supplementary Figure 5A). Differentiation of podocytes was induced by growing the immortalized podocyte cell line at non-permissive temperature 37° C in the absence of interferon- γ and was evident by the expression of synaptopodin that is specific for mature podocytes (Supplementary Figure 9). A different set of *Trpc* mRNA transcripts were expressed in the undifferentiated cells (at permissive temperature 33° C and with interferon- γ) (Supplementary Figure 5A). We focused on TRPC3 for potential interaction with TRPC6 because human *TRPC2* is a pseudo gene and that the role of TRPC5 in mediating ATP-induced Ca²⁺ entry in the present study is less likely due to the result of blocking by La³⁺ (see main Figure 1A). TRPC3 is closely related to TRPC6 and also directly activated by DAG (4). TRPC3 may form functional heteromultimers with TRPC6 in polarized epithelial cells (5). Because the very low abundance of TRPC3 in the mouse podocyte cell line (Supplementary Figure 5A), we examined the potential interaction between TRPC3 and TRPC6 using recombinant proteins expressed in HEK cells.

In cells co-transfected with Flag-TRPC3 and GFP-TRPC6, pull-down of TRPC3 by anti-Flag antibodies resulted in co-immunoprecipitation of TRPC6 (Supplementary Figure 5B). TRPC6 was not precipitated in cells without cotransfection with TRPC3. Because I-V relationship curves and biophysical properties of TRPC3 and TRPC6 are similar, it is difficult to distinguish between homomeric TRPC3 or C6 and heteromeric TRPC3/C6 channels in co-transfected cells. We therefore studied the regulation of TRPC3 by soluble klotho separately from TRPC6. Soluble klotho inhibited TRPC3 as well as TRPC6 (Supplementary Figure 5, C and D). As is for TRPC6, serum enhanced surface expression of TRPC3 and klotho prevented the enhancement of surface abundance by serum (Supplementary Figure 5E). Moreover, knockdown of VAMP2 decreased surface abundance of TRPC3 and prevented

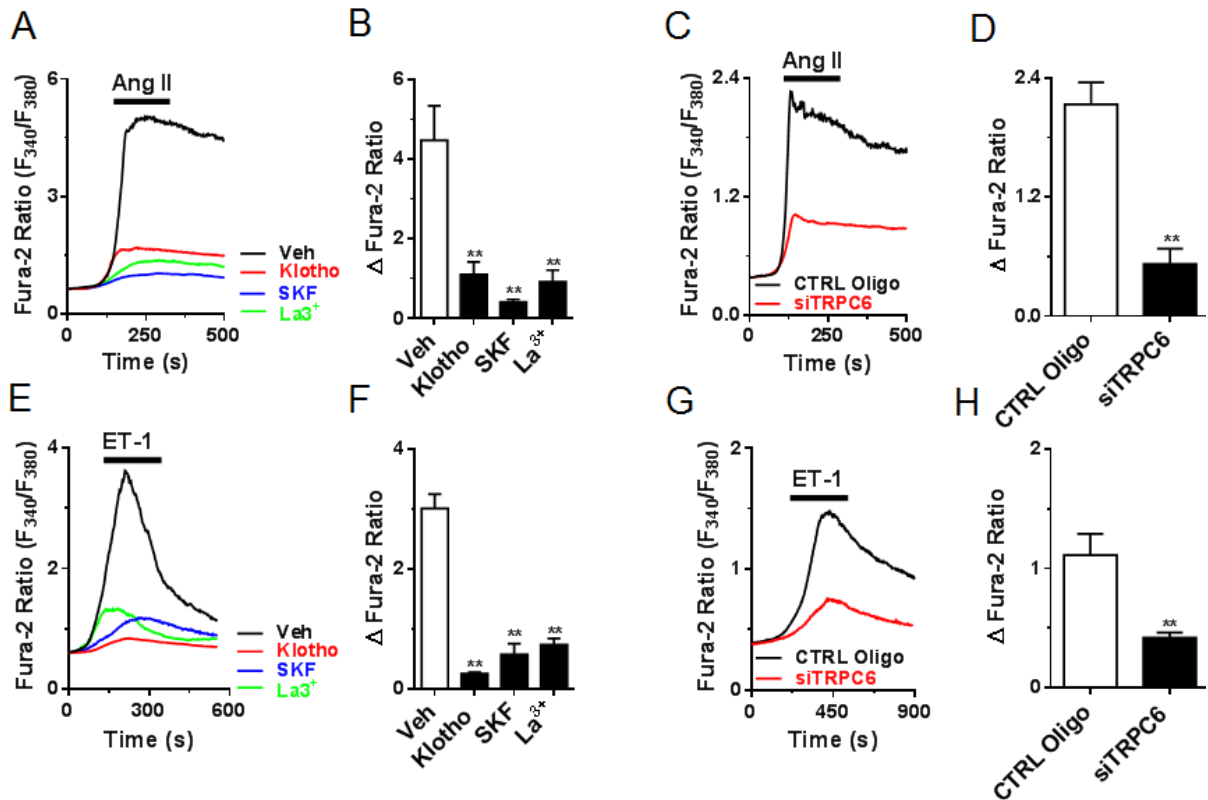
the downregulation of TRPC3 by klotho. Thus, the mechanism of klotho regulation of TRPC3 is similar to that of TRPC6. Overall, these data support the notion that soluble klotho downregulates heteromultimeric TRPC3/TRPC6 channels if they are present in podocytes.

References

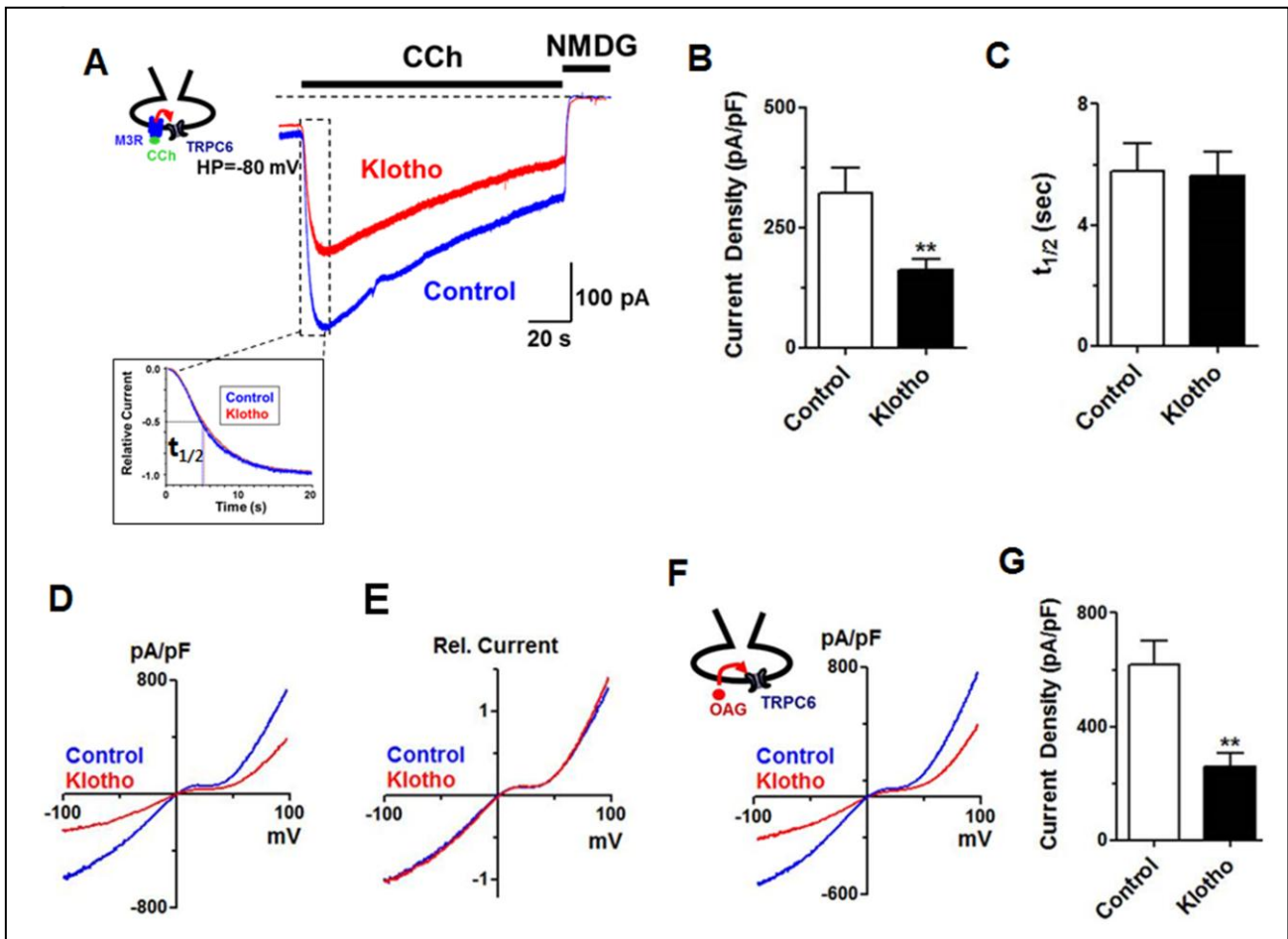
1. Sonthemier H, Ransom, C.B. In: Walz W, Boulton, A. A., Baker, G.B. ed. *Patch-clamp analysis advanced techniques*. Totowa, New Jersey, USA: Human Press; 2002:35-67
2. Xie J, Cha SK, An SW, Kuro OM, Birnbaumer L, Huang CL. Cardioprotection by Klotho through downregulation of TRPC6 channels in the mouse heart. *Nat Commun* 3:1238 doi:10.1038/ncomms2240, 2012
3. Strubing C, Krapivinsky G, Krapivinsky L, Clapham DE. Formation of novel TRPC channels by complex subunit interactions in embryonic brain. *J Biol Chem* 278(40):39014-13019, 2003
4. Hofmann T, Obukhov AG, Schaefer M, Harteneck C, Gudermann T, Schultz G. Direct activation of human TRPC6 and TRPC3 channels by diacylglycerol. *Nature* 397(6716): 259-263, 1999
5. Bandyopadhyay BC, Swaim WD, Liu X, Redman RS, Patterson RL, Ambudkar IS. Apical localization of a functional TRPC3/TRPC6-Ca²⁺-signaling complex in polarized epithelial cells. Role in apical Ca²⁺ influx. *J Biol Chem* 280: 12908-12916. 2005

Supplementary Table-1. Primer sequences for RT-PCR analysis

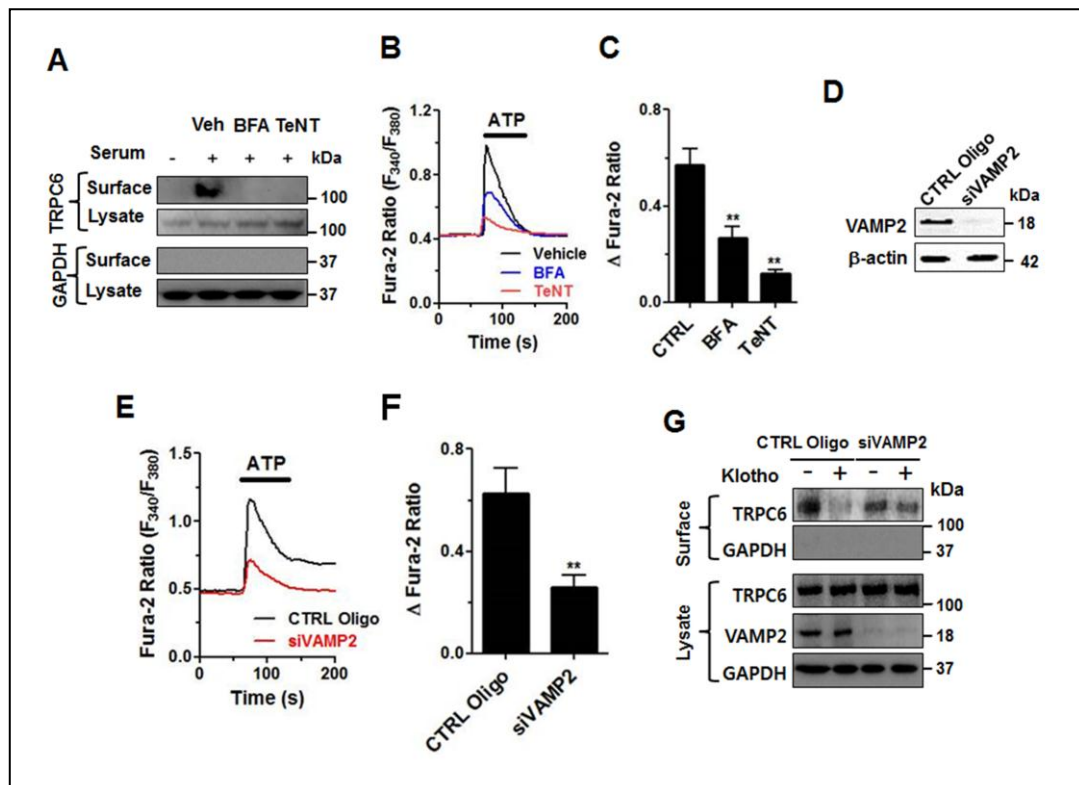
Target gene	Gene Bank Accession No.	Primer sequences
α -Klotho	NM_013823.2	F-5' AGCAATCAGACTGGATGGGGTC 3'
		R-5' GAGAGTAGTGTCCACTTGAACG 3'
β -Klotho	NM_031180.2	F-5' CCGCGTGTTTGGTTATACGGCC 3'
		R-5' CGGGCTTAAGAACAGACTCAGTG 3'
TRPC1	NM_011643.2	F-5' GATTTGCTCGCATACTCGAAAG 3'
		R-5' TGTCGCATGGACGTCAGGTAG 3'
TRPC2	NM_001109897.2	F-5' AGGGCCATGTACGGCATCTTTA 3'
		R-5' AGCGAGCAAACCTTCCACTCCA 3'
TRPC3	NM_019510.2	F-5' ATCTGGAAGTGGGCATGGGTAA 3'
		R-5' TGATATCGTGTTGGCTGATTGAGAA 3'
TRPC4	NM_016984.3	F-5' AACCTGGTGAAGCGGTACGTG 3'
		R-5' ACTTCGAAGCGGAAGCTAGAAATG 3'
TRPC5	NM_009428.2	F-5' GCAGCATTGTATGTGGCAGGA 3'
		R-5' CCTCGCCAAGGTTTCATCTGAC 3'
TRPC6	NM_013838.2	F-5' ACATCGGCTACGTTCTGTATGGTG 3'
		R-5' CAATTTGGCCCTTGCAAACCTC 3'
TRPC7	NM_012035.3	F-5' AACCTGACAGCCAATAGCACCTTC 3'
		R-5' TGGGCCTTCAGCACGTATCTC 3'
Synaptopodin	NM_177340.2	F-5' AAGGGTCTGACCTCATTGGA 3'
		R-5' GCAAAACCAAGGGCTACAAC 3'



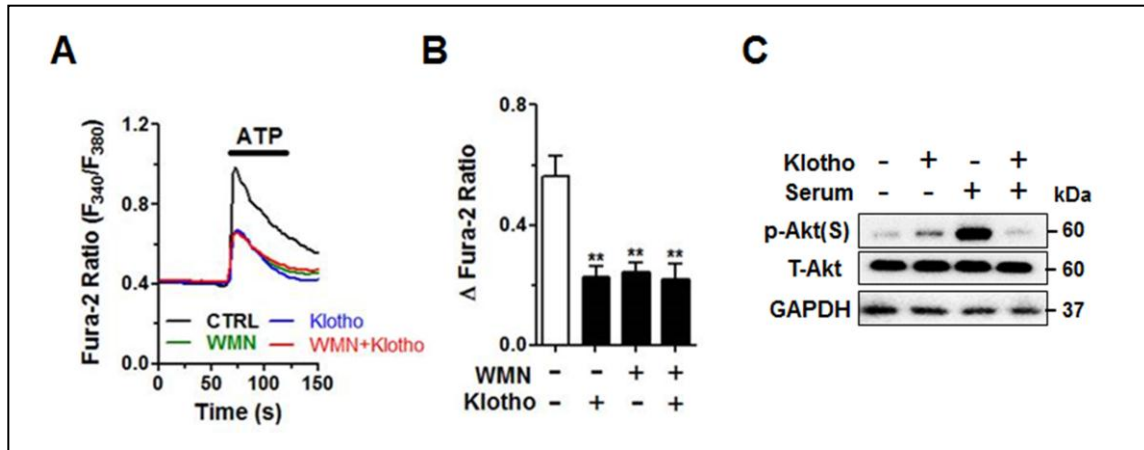
Supplementary Figure 1. Soluble klotho inhibits angiotensin II (Ang II)- and endothelin-1 (ET-1)-induced, TRPC6-mediated increases in $[Ca^{2+}]_i$ in cultured mouse podocytes. **(A)** Representative traces showing exposure to Ang II (1 μ M) caused an increase in $[Ca^{2+}]_i$ in cultured mouse podocytes. Preincubation of cells with SKF96365 (50 μ M, 1 hr) or La³⁺ (100 μ M, 1 hr) blunted the increases. **(B)** Summary of results in panel A. ** denotes $p < 0.01$ versus control (vehicle). **(C)** Representative traces showing Ang II-induced increases in $[Ca^{2+}]_i$ were reduced in cells transfected with siRNA against *Trpc6* vs control oligonucleotides. **(D)** Summary of results in panel C. ** denotes $p < 0.01$ vs control oligo (CTRL oligo). **(E)** Representative traces showing exposure to ET-1 (100 nM) caused an increase in $[Ca^{2+}]_i$ in cultured mouse podocytes. Preincubation of cells with SKF96365 (50 μ M, 1 hr) or La³⁺ (100 μ M, 1 hr) blunted the increases. **(F)** Summary of results in panel E. ** denotes $p < 0.01$ versus control (vehicle). **(G)** Representative traces showing ET-1-induced increases in $[Ca^{2+}]_i$ were reduced in cells transfected with siRNA against *Trpc6* vs control oligonucleotides. **(H)** Summary of results in panel C. ** denotes $p < 0.01$ vs control oligo (CTRL oligo).



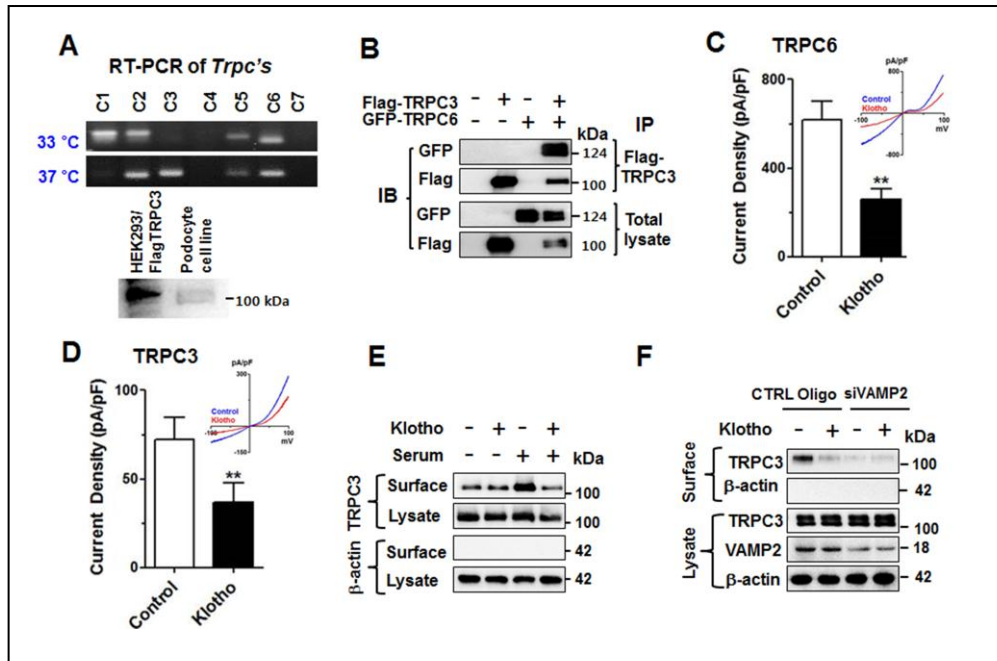
Supplementary Figure 2. Biophysical characterization of TRPC6 expressed in HEK cells with or without klotho. **(A)** Carbachol (CCh)-induced inward current (at -80 mV) through TRPC6 in HEK cells coexpressing M₃ muscarinic receptor (M₃R) and TRPC6 in the presence or absence of klotho. Inset shows time to maximal activation of superimposed relative currents in the presence or absence of klotho. **(B)** CCh-induced current density of TRPC6 (pA/pF at -100 mV) in the presence or absence of klotho. ** denotes $p < 0.01$ vs control. $n = 5$ each group. **(C)** Summary of half-time to maximal activation ($t_{1/2}$) of CCh-induced current in the presence or absence of klotho determined as shown in inset of panel A. $n = 5$ each group. **(D)** CCh-induced current-voltage relationship curves of TRPC6 in the presence or absence of klotho. **(E)** CCh-induced relative current-voltage curves of TRPC6 in the presence or absence of klotho. **(F)** OAG-induced current-voltage curves of TRPC6 in the presence or absence of klotho. **(G)** Summary of data as in panel G. ** denotes $p < 0.01$ vs control. $n = 6$ each group.



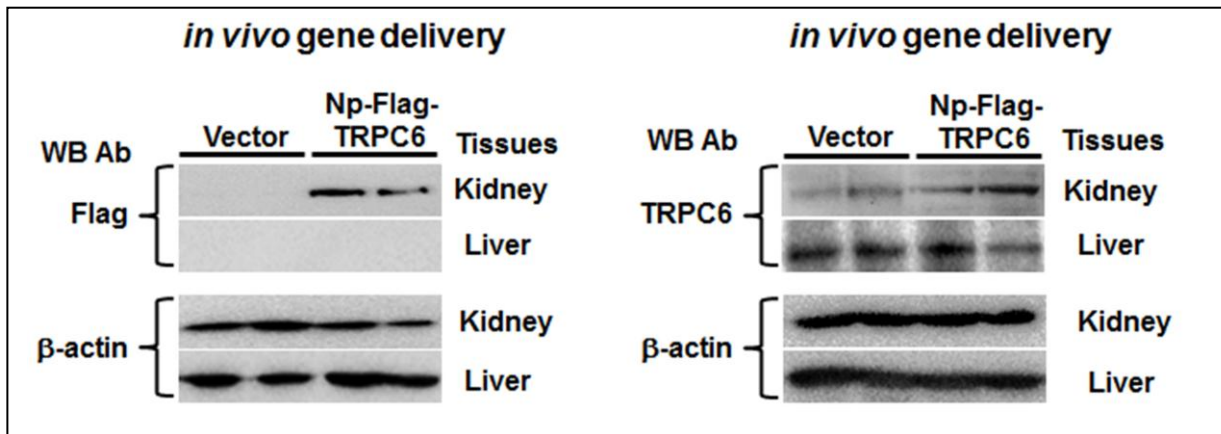
Supplementary Figure 3. Klotho reduces growth factor-dependent exocytosis of TRPC6 in podocytes. **(A)** Serum enhanced cell-surface expression of TRPC6, which was abrogated in cells treated with brefeldin A (BFA, 10 nM for 1 hr) or tetanus toxin (TeNT, 60 nM for 4-5 hr). Cell surface abundance of TRPC6 was measured by biotinylation assays. Experiments were repeated 2 times with similar results. **(B)** Representative traces illustrating treatment with BFA or tetanus toxin blunted ATP-induced increases in $[Ca^{2+}]_i$ (Δ Fura-2 ratio indicating difference in the ratio before and after ATP). **(C)** Summary of results in panel C. ** denotes $p < 0.01$ vs vehicle control. **(D)** Successful knockdown of Vamp2 in podocytes by siRNA (siVAMP2) was evident by western blot analysis. **(E)** Representative traces showing ATP-induced increases in $[Ca^{2+}]_i$ in podocytes transfected with control oligonucleotide (CTRL Oligo) or siRNA against VAMP2 (siVAMP2). **(F)** Summary of results in panel E. ** denotes $p < 0.01$ versus control oligo (CTRL oligo). **(G)** Soluble klotho decreased surface abundance of TRPC6, and the decrease was eliminated by knockdown of VAMP2. Experiments were repeated 3 times with similar results. $n = 5-7$ cells in each group in panel C and F.



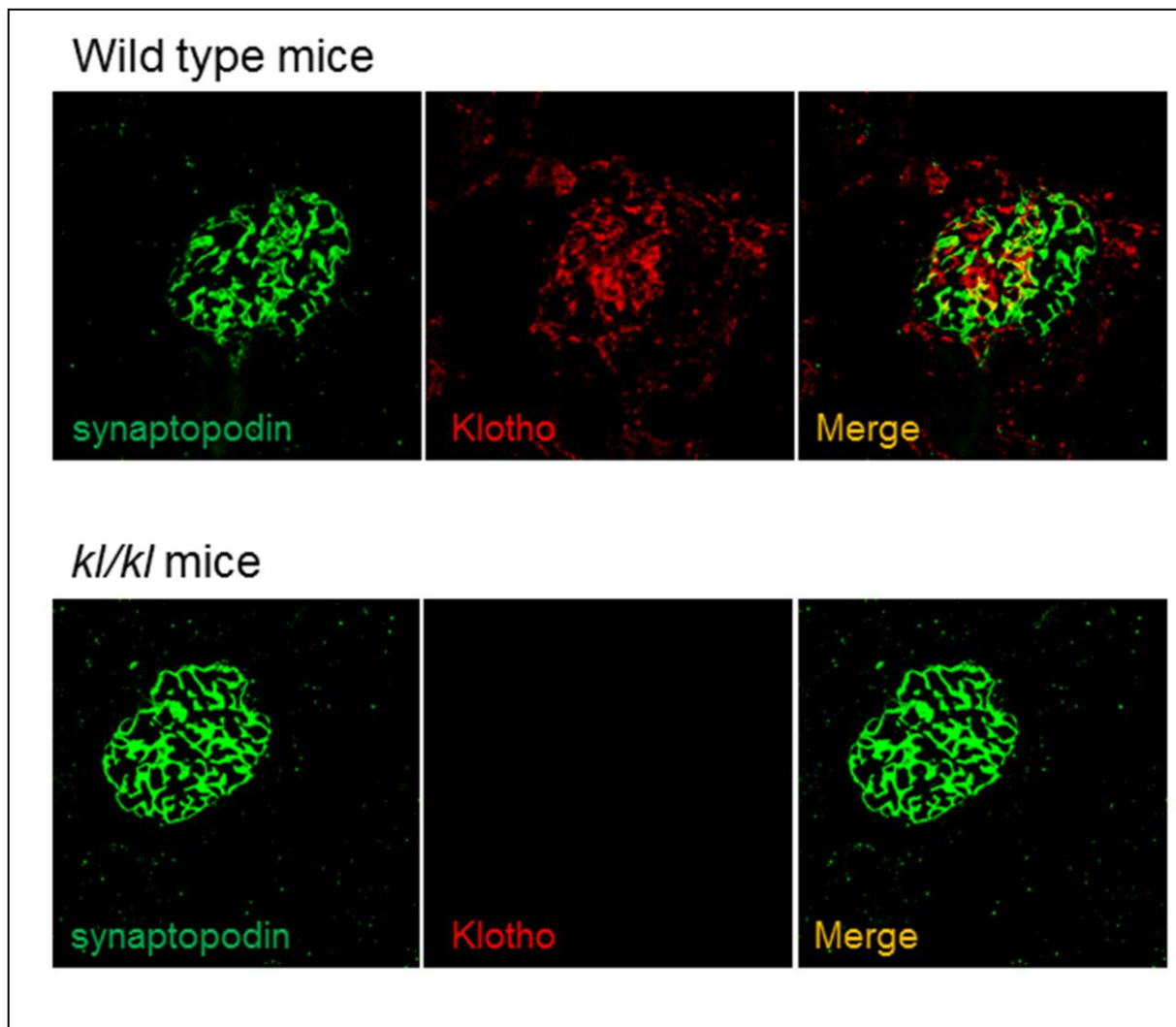
Supplementary Figure 4. Klotho inhibits PI3K and Akt-dependent exocytosis of TRPC6 in mouse podocytes. **(A)** Treatment with PI3K inhibitor wortmannin (WMN, 100 nM for 1 hr) inhibited ATP-induced increases in $[Ca^{2+}]_i$, and prevented the inhibition by klotho (500 pM for 1 hr). In experiments using WMN + klotho, cells were pretreated with WMN for 1 hr before addition of klotho and further incubation for 1 hr. **(B)** Summary of results in panel A. ** denotes $p < 0.01$ vs control oligo (without WMN or klotho). $n = 6$ cells in each group. **(C)** Effect of klotho on serum-induced Akt phosphorylation in cultured mouse podocytes. The abundance of phospho-Akt phosphorylated at serine-473 [p-Akt(S)] and total Akt (T-Akt) were shown, respectively. Cells were grown in serum-free or serum-containing medium, and treated with or without klotho. Experiments were repeated 3 times with similar results.



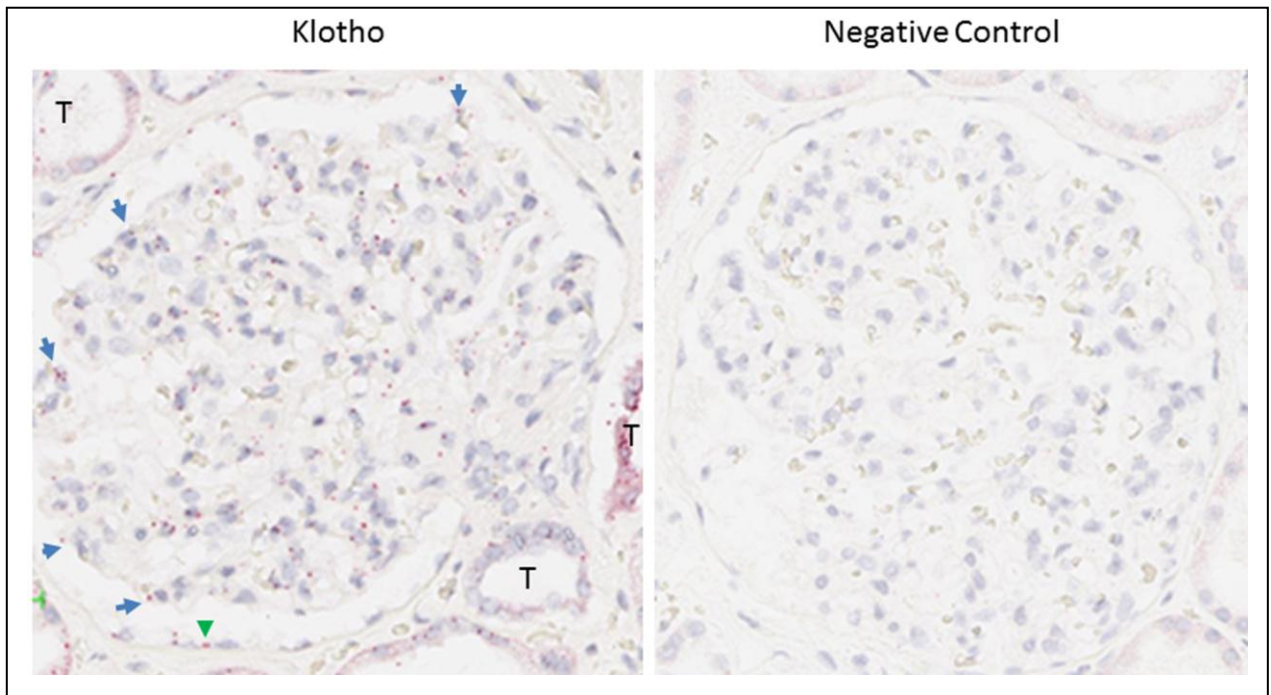
Supplementary Figure 5. Effect of klotho on TRPC3, which forms heteromultimers with TRPC6 in HEK cells. **(A)** Expression of *Trpc* isoforms analyzed in undifferentiated (at permissive temperature 33°C) and differentiated (at non-permissive temperature 37°C) mouse podocytes. Top panel shows mRNA analyzed by real-time polymerase chain reaction (RT-PCR). Bottom panel shows detection of TRPC3 protein in podocytes using recombinant TRPC3 expressed in HEK cells for comparison. **(B)** Co-immunoprecipitation of TRPC3 and TRPC6 expressed in HEK cells. Flag-tagged TRPC3 and GFP-tagged TRPC6 were co-expressed in HEK cells. Detergent-solubilized lysates were incubated with anti-Flag antibody to precipitate TRPC3. Co-precipitation of TRPC6 was detected by using anti-GFP antibody. Experiments were repeated 2 times with similar results. **(C)** Effect of klotho on TRPC6 expressed in HEK cells. Bar graph shows mean \pm SEM current density (pA/pF at -100 mV) of TRPC6 recorded by whole-cell recording. $n = 6$ cells in each group. Inset shows I-V curves. ** denotes $p < 0.01$ vs control without klotho. **(D)** Effect of klotho on TRPC3 expressed in HEK cells. Bar graph shows current density (pA/pF at -100 mV) of TRPC3 recorded by whole-cell recording. $n = 6$ cells in each group. Inset shows I-V curves. ** denotes $p < 0.01$ vs control without klotho. Experiments were repeated 2 times with similar results. **(E)** Serum enhanced surface abundance of TRPC3 expressed in HEK cells and klotho prevented the enhancement. **(F)** Knockdown of VAMP2 decreased surface abundance of TRPC3 expressed in HEK cells, and prevented the inhibition by klotho. Experiments were repeated 3 times with similar results.



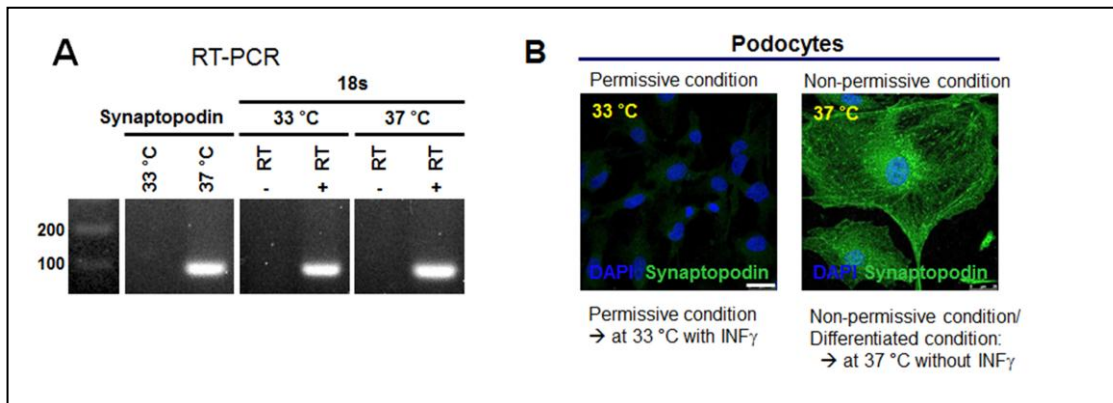
Supplementary Figure 6. Western blot analysis of exogenous Flag-TRPC6 protein and endogenous TRPC6 from kidney cortex and liver extracts 48 hr after *in vivo* gene delivery. *In vivo* hydrodynamic delivery of *Trpc6* gene was achieved by injection via tail-vein of plasmid encoding podocyte-specific Flag-tagged TRPC6 (“Np-Flag-TRPC6”) or empty pCDNA3 vector in 2 ml isotonic saline. Western blot analysis of exogenous Flag-TRPC6 was performed by using anti-Flag antibody (left panel), and of both exogenous and endogenous TRPC6 by anti-TRPC6 antibody (right panel), respectively.



Supplementary Figure 7. Cryosectioned kidney tissues from wild-type and homozygous *klotho*-hypomorphic mice were stained by goat anti-synaptopodin (green) and rat monoclonal anti-klotho (KM2076) (red) antibodies, respectively.



Supplementary Figure 8. *In situ* hybridization to detect klotho mRNA in normal human glomerulus. Normal kidney tissue from nephrectomy for renal cell carcinoma. Purple-red color dots indicate *Klotho* mRNA signals, which are present in podocytes (blue arrows), parietal epithelial cells (green arrowhead) as well as in renal tubules (labeled “T”). ISH was performed and detected by using highly sensitive commercial probe (The Advanced Cell Diagnostics, Inc. RNAscope® Probes). In the negative control, the probe used is a bacterial gene (*Dapb*), which is the recommended and currently well accepted method to demonstrate non-specific background.



Supplementary Figure 9. Differentiation of immortalized mouse podocytes in non-permissive condition (37°C and without interferon- γ). Expression of synaptopodin in differentiated cells evident by RT-PCR (**A**) and by immunofluorescent staining (**B**).